Bedrock Depth Calculation of Çanakkale (Turkey) Basin Using Rayleigh Ellipticity and Microgravity Survey

Aydın Büyüksaraç[1] , Onur Eyisüren[2] , Özcan Bektaş*[3] and Öznur Karaca[4]

Abstract

It is a well-known fact that the local ground effect plays an important role in the damage to structures during earthquakes. In order to define the soil-structure interaction correctly, the geometry of the tight and loose soil layers in the soil should be well known. In addition, the impedance contrast due to local ground effects can be deeper than the first 30 m, which is accepted as the engineering depth, and in this case, the Vs,30 parameter is disabled. For this reason, the location of engineering bedrock and seismic bedrock gains importance. The variation of shear wave velocity with depth is a key parameter for seismic field effect estimation. In addition, the separation of low-density layers close to the surface and higher-density bedrock can be easily done by the gravity method. Bedrock/seismic foundation levels were determined by using these two methods together for Çanakkale soils, which are known to have thick alluvial thickness and liquefaction problems. Microgravity measurements were made at 100 points and the anomalies obtained were modelled in three dimensions. In light of the data obtained from this study, it has been determined that the thickness of the loose basin unit in the study area is in the range of about 50-300 m. Ambient vibration was recorded with the help of a velocity seismometer at 146 points, and S velocity (Vs) profiles were obtained by using the inversion of the observed ellipticity curve. In addition, the velocity-depth change rate structure of the basin is defined depending on the Vs velocities on the 2D gravity model made along the two profiles that cut the basin in N-S and E-W directions. Along these profiles, the frequency range has been determined as 0.8-1.3 Hz in the deep parts of the Basin and 1.5-11.0 Hz in the shallow parts.

Resumen

Es bien conocida la importancia de los efectos locales del suelo en el daño a estructuras por sismos. Para definir correctamente la interacción suelo-estructura, es necesario establecer la geometría de las capas compactas y sueltas del suelo. Además, el contraste de impedancias debido a efectos locales del suelo puede exceder los 30 m de profundidad, que es la profundidad aceptada en ingeniería, y por ello, en este caso, se deshabilita el parámetro Vs,30. De allí la importancia de ubicar el lecho rocoso de ingeniería y el lecho rocoso sísmico. La variación de la velocidad de la onda de corte con la profundidad es un parámetro clave para la estimación del efecto de campo sísmico. Además, la separación de capas de baja densidad cercanas a la superficie del lecho rocoso de mayor densidad se puede realizar rápidamente mediante el método de gravedad. Para los suelos de Çanakkale, que tienen problemas de licuefacción y espesor aluvial grueso, los niveles de lecho rocoso/cimentación sísmica se determinaron usando ambos métodos. Las mediciones de microgravedad se realizaron en 100 puntos y se modelaron las anomalías obtenidas en tres dimensiones. A la luz de los datos obtenidos de este estudio, se determinó que el espesor de la unidad de material suelto en la cuenca del área de estudio está en el rango de aproximadamente 50-300 m. La vibración ambiental se registró con un sismómetro (sensor de velocidad) en 146 puntos, y los perfiles de velocidad S (Vs) se obtuvieron de la inversión de la curva de elipticidad observada. Además, la estructura de tasa de cambio de la velocidad con la profundidad en la cuenca se definió en función de las velocidades Vs en el modelo de gravedad 2D a lo largo de dos perfiles que cortan la cuenca en las direcciones N-S y E-W. A lo largo de esos perfiles, el rango de frecuencias se ha determinado de 0.8 a 1.3 Hz en las partes profundas de la Cuenca y de 1.5 a 11.0 Hz en las partes someras.

Editorial responsibility: Anonymous

* Corresponding author: Özcan Bektaş obektas@cumhuriyet.edu.tr
[1] Çan Vocational School, Çanakkale Onsekiz Mart University, TR-17400 Çan/Çanakkale, Turkey. e-mail:absarac@comu.edu.tr
[2] School of Graduate Studies, Çanakkale Onsekiz Mart University, TR-17020 Çanakkale, Turkey. e-mail: onureyisuren@gmail.com
[3] Department of Geophysical Engineering, Sivas Cumhuriyet University, TR-58140 Sivas, Turkey. e-mail:obektas@cumhuriyet.edu.tr
[4] Department of Geological Engineering, Çanakkale Onsekiz Mart University, TR-17020 Çanakkale, Turkey. e-mail:oznurkaraca@comu.edu.tr

A. Büyüksaraç, O. Eyisüren, Ö. Bektaş, Ö. Karaca

Introduction

While determining the behaviour of a site during the earthquake occurrence, it is generally acted according to the ground information near the surface. However, shallow and deep ground structures of that area must be well known to fully define the ground behaviour of a site. In particular, the distance of the near-surface soils to the bedrock is one of the most important factors that determine the ground behaviour during an earthquake occurrence. The depth of the bedrock and the presence of soft-medium solid clay deposits or liquefiable soils with low shear wave velocity on them and the inclusion of basin effects increase the PGV values and extend the period of the acceleration spectra.

Urban settlements generally develop towards looser, unstable, in other words, lowland regime areas in Turkey. For this reason, the foundation designs of buildings in urban settlements are made in areas with soil structure. This situation brings engineering problems that need to be solved at the design stage. In particular, the soil thickness under the buildings is very important information and factor in terms of defining the response of the site in terms of construction. For this reason, it is also important to determine the depth where the soil completely passes into the rock ambient (bedrock) or S-wave velocity reaches $600\text{-}760\,ms^{-1}$. The damage caused by the earthquakes that took place in Turkey in the last 25 years has revealed how important it is to know the underground model and the basin effect, too. On the other hand, it is imperative to generate the bedrock depth information to obtain a complete ground structure model in basin-type structures and to model information such as possible soil amplification and acceleration distribution. For this purpose, many studies have been carried out to obtain bedrock depth with experimental relations from inversion based on ambient vibration measurements (Delgado *et al.*, 2000a; Hinzen *et al.*, 2004; García-Jerez *et al.*, 2006; D'Amico *et al.*, 2008; Birgören *et al.*, 2009; Özalaybey *et al.*, 2011; Harutoonian *et al.*, 2013; Fairchild *et al.*, 2013; Del Monaco *et al.*, 2013; Mendecki *et al.*, 2014; Kuo *et al.*, 2016; Sant *et al.*, 2017; Molnar *et al.*, 2018; Liang *et al.*, 2018; Moon *et al.*, 2019; Thabet, 2019; Anbazhagan *et al.*, 2019; Rupar and Gosar, 2020; Büyüksaraç *et al.*, 2021; Magnami *et al.*, 2021).

Seismic microzonation or multi-parameter microzonation studies based on the inversion of surface waves have been carried out for many residential areas in Turkey. In these studies, ground motion parameters, site conditions, and their effects were evaluated using different soil classifications, and especially the surface and near-surface changes of soils were zoned (Över *et al.*, 2011; Büyüksaraç *et al.*, 2013; Akkaya and Özvan, 2019; Bekler *et al.*, 2019). In multi-parameter microzonation studies, a kind of risk ranking was carried out by evaluating multiple data within the framework of selected criteria (Kolat *et al.*, 2006). Later, when it was understood that this layer was especially effective on the bedrock or seismic bedrock, where the effect of amplifying the earthquake ground motion of the unstable ground sections was important, studies were developed to obtain V_s velocity measurements for the foundation limitation. The variation of regional S-wave velocity with depth and the bedrock, and depth distribution play an important role in the estimation of seismic hazard and earthquake ground motion characteristics in terms of understanding the seismic wave amplification potential of geological formations (Birgören *et al.*, 2009). Kamalian *et al.* (2008) mentioned the seismic bedrock in their study for the city of Qom, Iran, defined the levels that reached 760 m/s, and examined the behavior of the earthquake ground motion above this level. Similarly, Nakamura (2000) defined the S-velocity value of 600 m/s as the seismic basis. Especially in the upper part of this level, it was emphasized in most studies that the damage rate increased in the ground parts close to the surface.

Çanakkale is an area with a very high earthquake risk due to the earthquake sources around it (Figure 1). The ground structure of Çanakkale, which is quite loose and unstable, shows ground characteristics under the influence of shallow groundwater, and most importantly, it is known that there is not enough information about the depth of the bedrock. Site surveys within the boundaries of Çanakkale central zoning were completed within the scope of some projects in 2014. In this context, shallow soil structure and behavior were determined by single station microtremor and seismic MASW method. On the other hand, many researchers have conducted studies to determine the earthquake behavior, soil classification, and problems of shallow soil structure in the study area (Tunusluoğlu and Karaca, 2018; Bekler *et al.*, 2019; Büyüksaraç *et al.*, 2021).

Geophysical studies covering two different methods were carried out to eliminate this deficiency and to calculate the bedrock or seismic bedrock depth in the section between Karacaören and Kepez Plains, where Çanakkale central settlement is located within the scope of this study. First, microgravity measurements were made to determine the density contrast between loose and hard units. Considering that the volcanic units in the east of the Çanakkale Basin may be the basement rock, three-dimensional modeling has been made. Then, the V_s velocity structure was obtained from the measurements based on the ambient vibrations in the environment. Compatibility analysis was made by comparing the results obtained with both methods and the ground structure was defined on the two-dimensional models.

Seismicity and Seismotectonic of Çanakkale Basin

The Biga Peninsula, where the Çanakkale Basin is located, is one of the most active parts of the North-West Anatolian seismotectonic regime dominated by a strike-slip structure

bounded by normal or oblique faults (McKenzie, 1978; Şengör *et al.*, 1985; Barka *et al.*, 1997; Kürçer *et al.*, 2008; Ateş *et al.*, 2009; Le Pichon and Kreemer, 2010; Fairchild *et al.*, 2013). Çanakkale city, which is our study area, is located in Northwest Anatolia, in other words, in the northern Aegean Region. The Biga Peninsula, to which Çanakkale belongs geographically, is in the southern part of the North Anatolian Fault Zone (*NAFZ*), the most important fault zone in Turkey. When the distribution of earthquakes in and around Çanakkale is examined, four sub-seismic zones can be mentioned. These are *NAFZ* in the north, the Yenice-Gönen Fault Zone (*YGFZ*) in the east, and the Ganos Fault (*GF*), which is the continuation of the *NAFZ* in the north, in the northwest, respectively. The most important active fault that may affect the study area is the Ganos Fault along the Gaziköy-Gölcük-Kavakköy line, two of the most active fault systems in Southern Marmara, and the SW-NE trending Yenice-Gönen Fault Zone. These faults are approximately 50 km away from the study area. (Figure 1). On the other hand, Çanakkale is affected by all earthquakes in the Aegean Sea. As can be seen from the map given in Figure 1, Çanakkale is under the influence of seismogenic zones that produce devastating earthquakes. When the historical records are examined, it is understood that the ancient settlement, especially known as the ancient city of Troy, was destroyed and rebuilt 9 times. Therefore, information such as soil thickness and soil behaviour become much more important for such areas.

Geology Of Çanakkale And Its Surroundings

The main geological elements of the Biga Peninsula are Metamorphic rocks, Ophiolites, Neogene basin sediments, and Magmatic rocks that started from the Oligo-Miocene and continued their development at intervals until the Quaternary (Siyako *et al.*, 1989). Paleozoic or possibly older metamorphic rocks form the basement of the Biga Peninsula (Kazdağ Group). Over the metamorphic rocks, there is the Triassic aged Karakaya Complex, which consists of different tectonostratigraphic units represented by active continental margin deposits with a tectonic contact (Figure 2). In the Upper Cretaceous, the Çetmi ophiolitic mélange was emplaced in the region with a complex and irregular internal structure mainly composed of spilite, greywacke, pelagic shale, serpentinite and radiolarites. The products of the acidic magmatism active in various stages in the Biga Peninsula are mostly granite, granodiorite and diorite compositions. Researchers studying in the region in the previous years (Birkle and Satır, 1995; Genç and Yılmaz, 1994) discovered the Kestanbol, Evciler, Karaköy and Eti plutons, the product of Tertiary magmatism and the Biga defined as shallow intrusions formed due to Lower Miocene volcanism in the

peninsula. Plutons are NE-SW long axis elliptical igneous masses and they are surrounded by fine-grained volcanic rocks of similar composition (Karacık and Yılmaz, 1998). Çanakkale Group is located on older polygenic basement rocks with angular unconformity.

The formations in the Çanakkale Group are located on both sides of the Dardanelles Strait and from bottom to top consist of four litho-stratigraphic units including "Gazhanedere fm., Kirazlı fm., Çamrakdere fm. and Alcitepe fm.". From a stratigraphical point of view, the lowest levels of the Çanakkale Group are composed of the Gazhanedere formation, which was deposited in a terrestrial environment and represented by conglomerate, sandstone and mudstone, aged between the Middle Miocene and the beginning of the Late Miocene. The mudstone-supported conglomerate is loosely cemented and locally mud conglomerate. The Gazhanedere formation typically reflects the alluvial fan in terms of facies features and deposition geometry. The transition of the unit into fine-grained lithologies towards the coarse-grained basin at the basin margins indicates the alluvial fan environment (Atabey *et al.*, 2004). The longitudinal and/or transverse bar deposits found in it indicate that this spectrum developed in a braided river environment, and many depositional structures such as the indeterminate thick layer, the presence of cross layers, and the presence of wedged layers in places indicate that this environment is irregular and high-energy. The presence of red mudstones in it indicates both terrestrial formation and flood plain.

The Kirazlı formation is mostly composed of fine-coarse grained sandstone and lesser amounts of fine conglomerate, siltstone and mudstone. It was deposited in coastal and near-shore (coast, beach, tidal delta) environments. It is widely observed in the study area. The Kirazlı formation is a loosely anchored unit dominated by sandstones deposited in near-coastal environments. Among the sandstones, siltstone, claystone intercalations and conglomerates in the form of channel fillings are rarely observed. The thickness of the formation varies from region to region. It is approximately 220 m in type section near Kirazlı Village. Şentürk and Karaköse (1987) measured 132 m around Intepe, 157 m in Bayrak Tepe and 204 m in Çamrakdere. They stated that the thickness of the Gallipoli Peninsula could reach up to 500 m. The Kirazlı formation is transitional with the Gazhanedere formation at the bottom and the Çamrakdere and Alçıtepe formations at the top (Siyako, 2006).

Çamrakdere formation is transitional with Kirazlı formation at the bottom and Alçıtepe formation at the top (Siyako, 2006). The dominant lithology in the unit is mudstone-claystone and consists of siltstone, sandstone, conglomerate with pebbles and calcarenite. The claystone-mudstone layers of the unit play a primary role in the development of the landslides
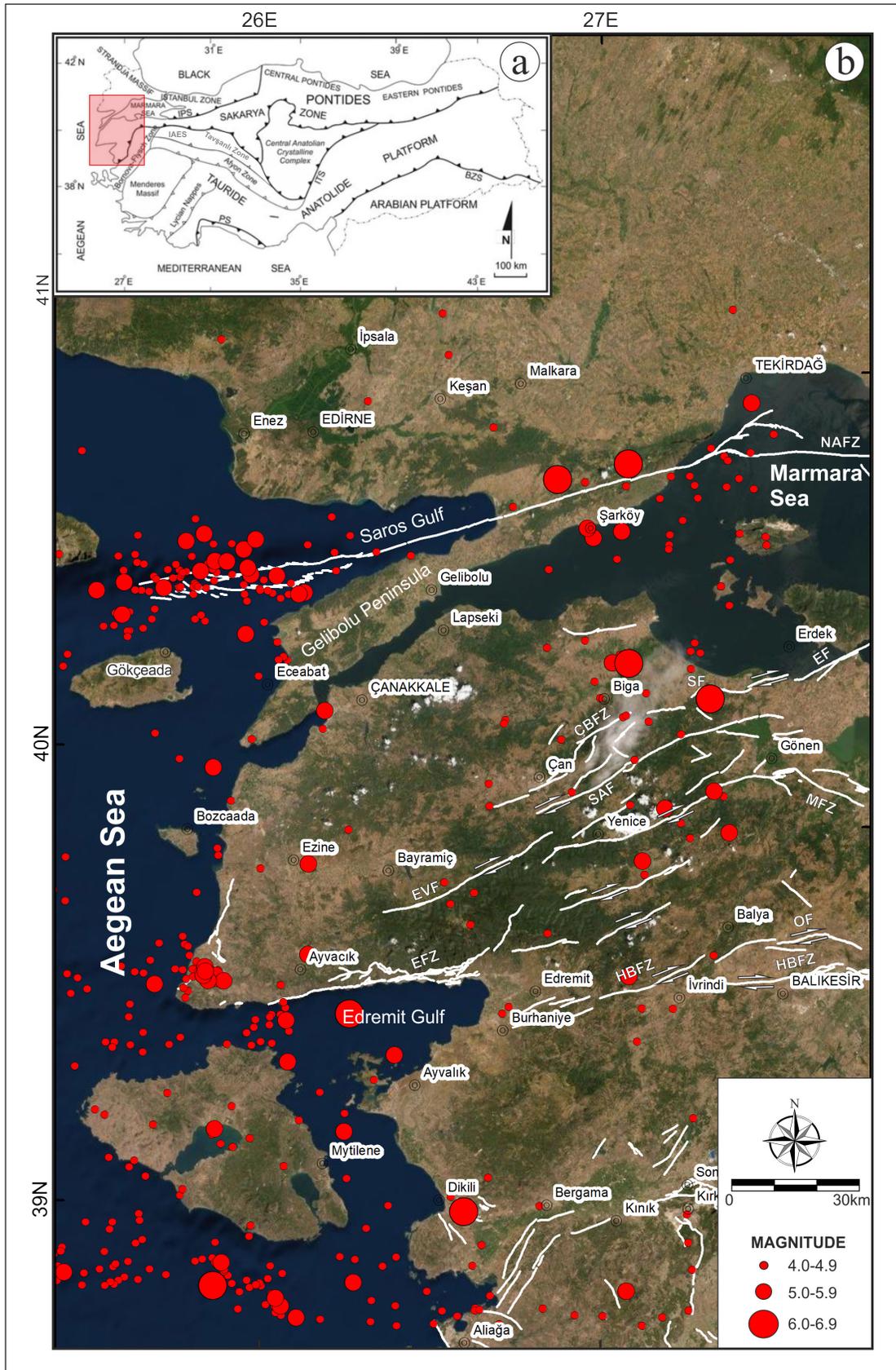
Figure 1 (a). Tectonic Units of Turkey. Red rectangular box shows the study area, (b) Epicentral distribution (between 1900 and 2021 years for M ≥ 4.0) and faults of Biga Peninsula and its environment. *NAFZ*: North Anatolian Fault Zone, *GF*: Ganos Fault, *CBFZ*: Çan-Biga Fault Zone, *SAF*: Sarıköy Fault, *YGFZ*: Yenice-Gönen Fault Zone, *SF*: Sinekçi Fault, *EF*: Edincik Fault, *EVF*: Evciler Fault, *MFZ*: Manyas Fault Zone, *EFZ*: Edremit Fault Zone, *HBFZ*: Havran-Balya Fault Zone, *OF*: Ortaca Fault

observed in the region. The formation was measured as 55 m at Bayrak Tepe near Çanakkale and 222 m at Çamrakdere in Lapseki district (Siyako, 2006).

The Alçıtepe Formation starts with beige-gray coloured, medium bedded, pebbly and sandy carbonates at the base, transitioning with the clastics of the Çamrakdere Formation. The units that make up the formation are mudstone, marl, siltstone, sandstone, calcite and fine conglomerate. These lithologies are laterally and vertically transitive with each other. It can be seen in the military area around Narababa Hill, in the area where Esenler District is located and around the Barbaros Martyrdom.

The Alçıtepe formation consists of alternations of sandy limestone, sandstone, claystone, marl and limestone with abundant macrofossils and oolitic limestones (Siyako, 2006). The Alçıtepe formation was deposited in a mixed, clastic-carbonate shoreline environment consisting of coastal and offshore clastics and carbonates (Şentürk and Karaköse, 1987). The fact that it contains lagoonal sediments fed by

rivers at the bottom and oolitic limestones consisting of turbulent shoreline and offshore sediments at the top indicates that the unit was deposited not only beyond the coast, but also in an area along the clastic coastline. The repetition of clastic sediments and carbonate sediments at some levels indicates that the coastline is volatile (moving) (Şentürk and Karaköse, 1987).

Alluviums consisting of unconsolidated sediments are very common in the study area. Both the distribution and formation of these alluviums took place under the influence of Sarıçay. Sarıçay collects the sediments it carries from high elevations, both along its old bed and along its new bed, primarily at low-lying plains. These deposits are grouped into three separate units according to their formation forms and the locations of the lithology types that compose them (Figure 3). 1st group, sand, clayey sand, partially gravel channelled sand unit, 2nd group, sand, silty sand unit, and 3rd group, block, gravel and sand (existing riverbed and floodplain sediments) unit (Büyüksaraç *et al.*, 2022). As you
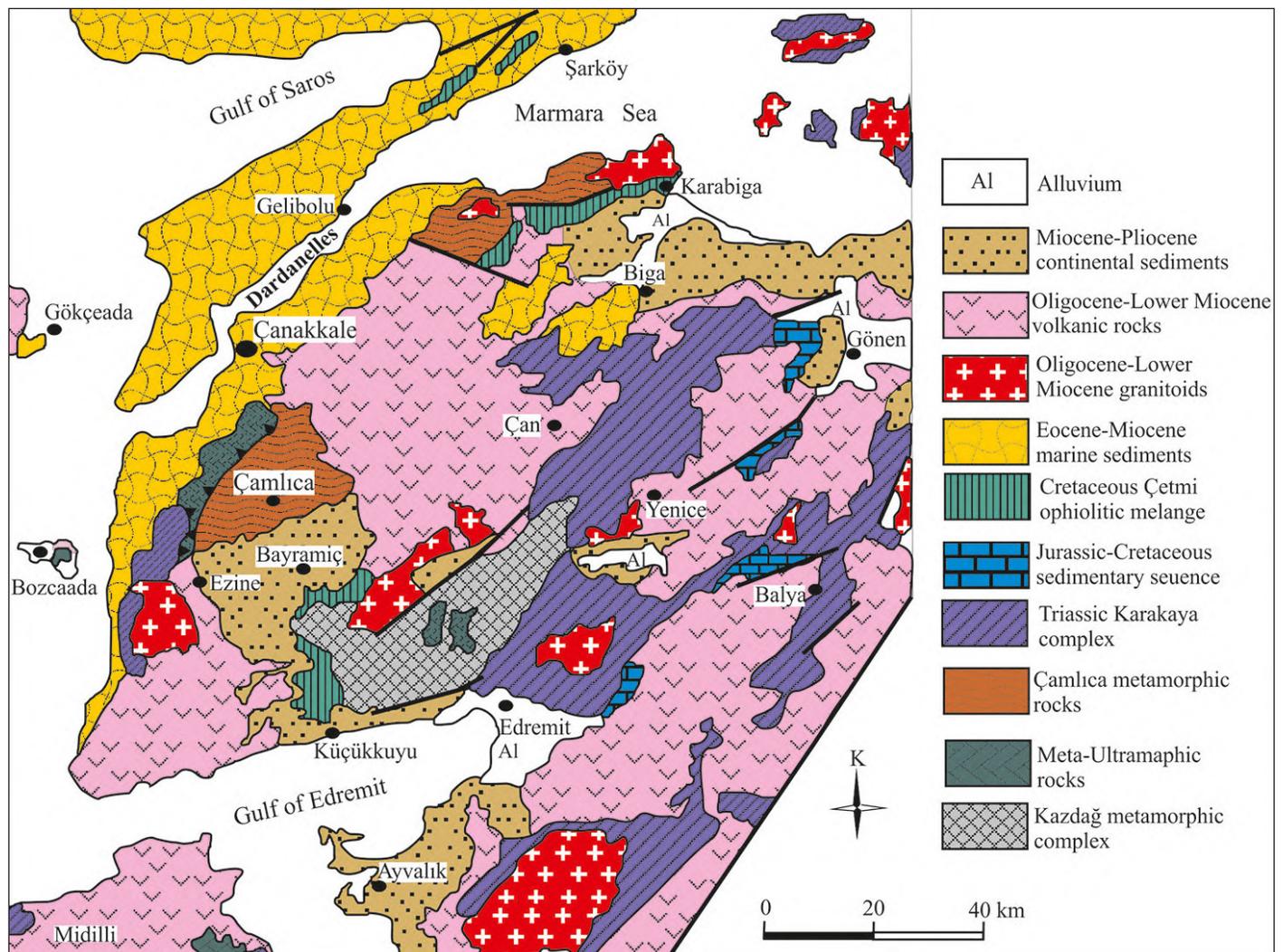
Figure 2. Geological map of Çanakkale and its surroundings, including the Biga and Gallipoli peninsulas (Atabey *et al.*, 2004; Duru *et al.*, 2012; Ilgar *et al.*, 2008; 2012; Yiğitbaş, 2016).

move away from the main bed of Sarıçay, the grain size in the sediments decreases, and block gravel, sand, silt and clay elements show lateral and vertical transitions with each other.

3D Bedrock Depth Map of Çanakkale Basin Based on Gravity Data

Gravity data were collected with the grid network created in an area of approximately 10×10 km, that aims to reach the borders of the Çanakkale basin, which includes the study area and its surroundings (Figure 4). The distance between profiles and measurement points was equal and taken as 1 km. Field data collection protocols were carried out by making 60-second, 5-repetitive measurements at 100 stations using the Scintrex CG-5 gravimeter.

In addition, a base measurement was made averagely every 2 hours to control the instrumental drift at 4 temporary base stations. After the raw data set is obtained, free air,

latitude, Bouguer and terrain corrections are required for correction of data in gravity measurements. However, this correction was not made because the topographic change was insignificant in the study area. Other corrections were made, and the Bouguer gravity anomaly map of the study area was prepared. Station locations were determined using high precision d-GPS.

Gravity data are reduced to complement the Bouguer anomalies using a reduction density of $2.58\,g.cm^{-3}$. Figure 5a shows the Bouguer gravity map of the study area obtained by gridding the reduced data. In the Bouguer gravity map, there are high gravity values in the low middle part of the area in the north and south of the area. The height measurements made during the survey were also used for the necessary information to make the altitude correction to the microgravity measurements. The elevation information obtained was mapped and the elevation change in the area
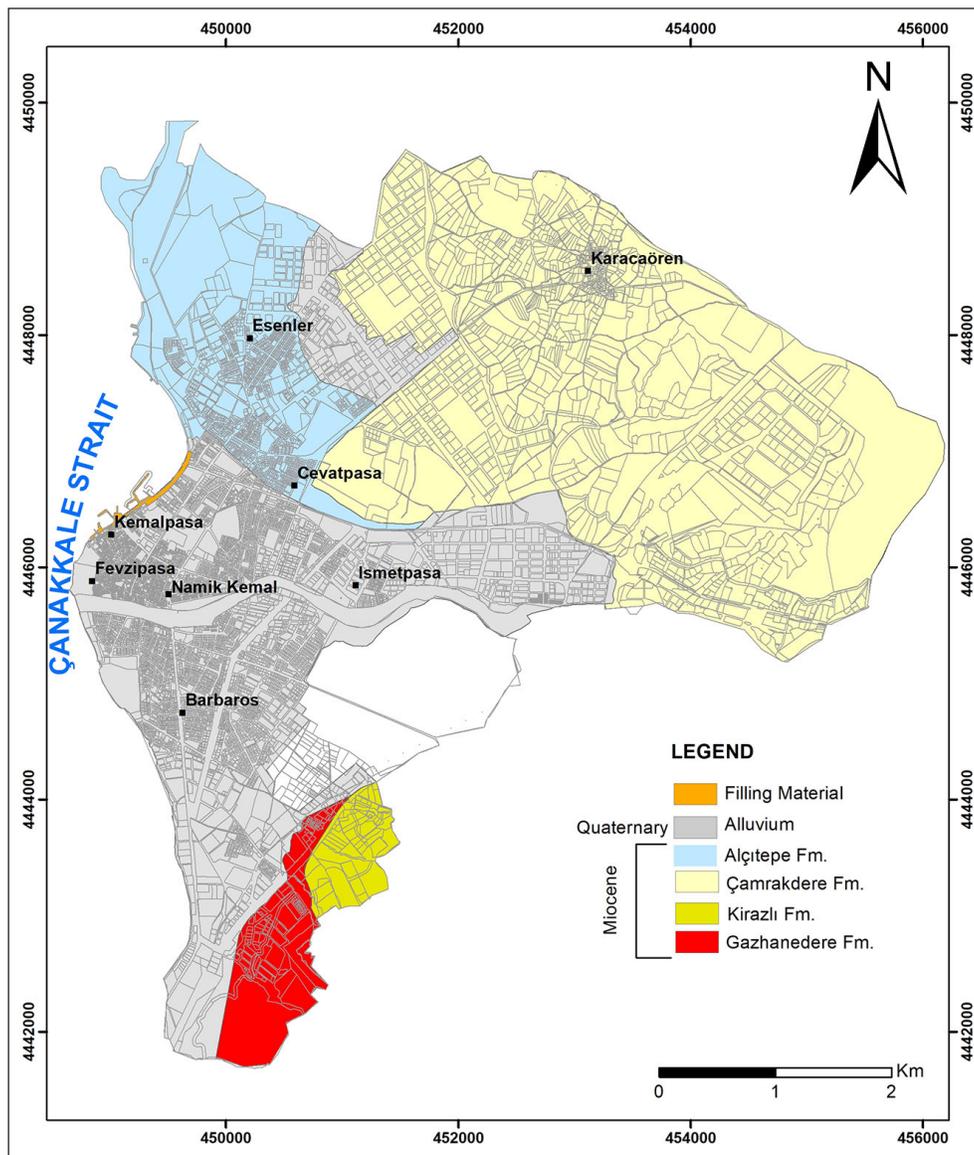
Figure 3. Geological map of the study area (Büyüksaraç *et al.*, 2022).
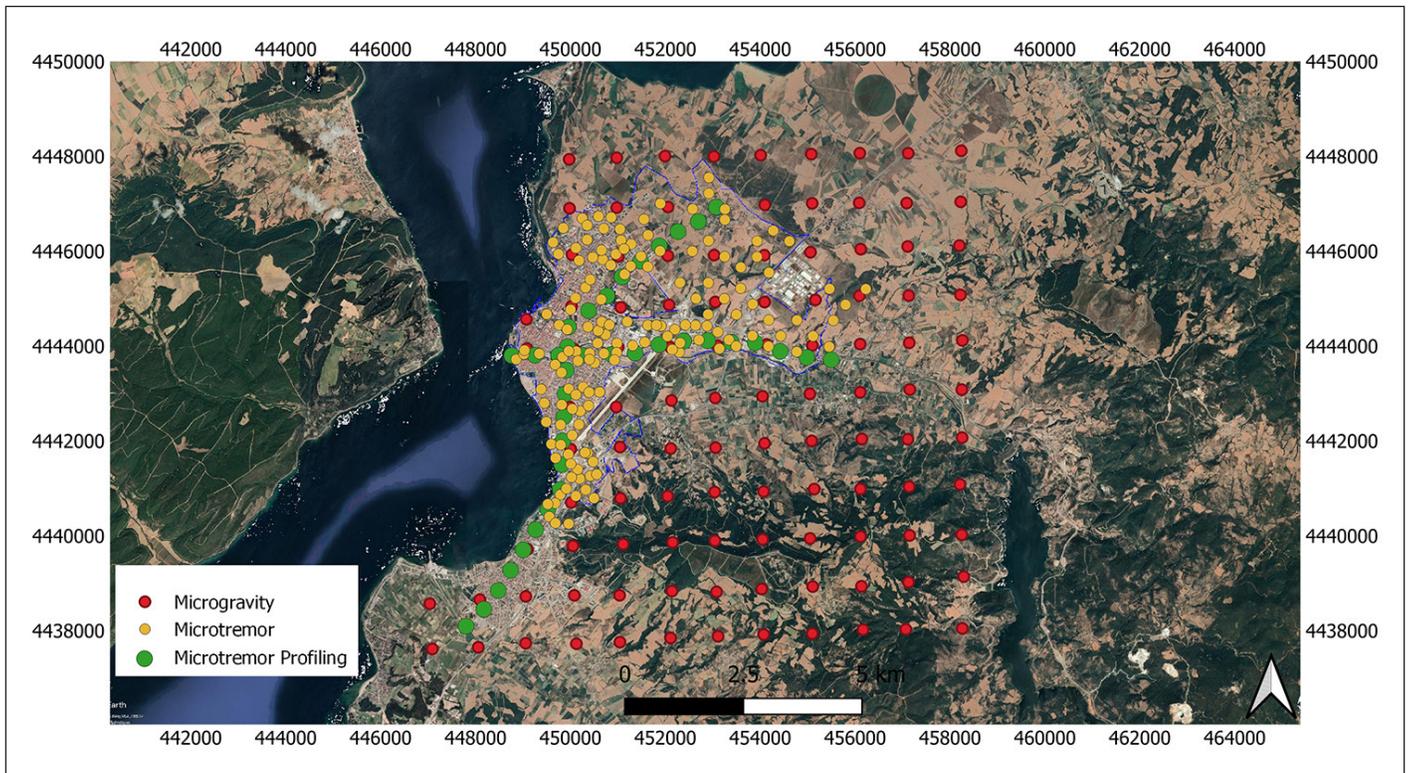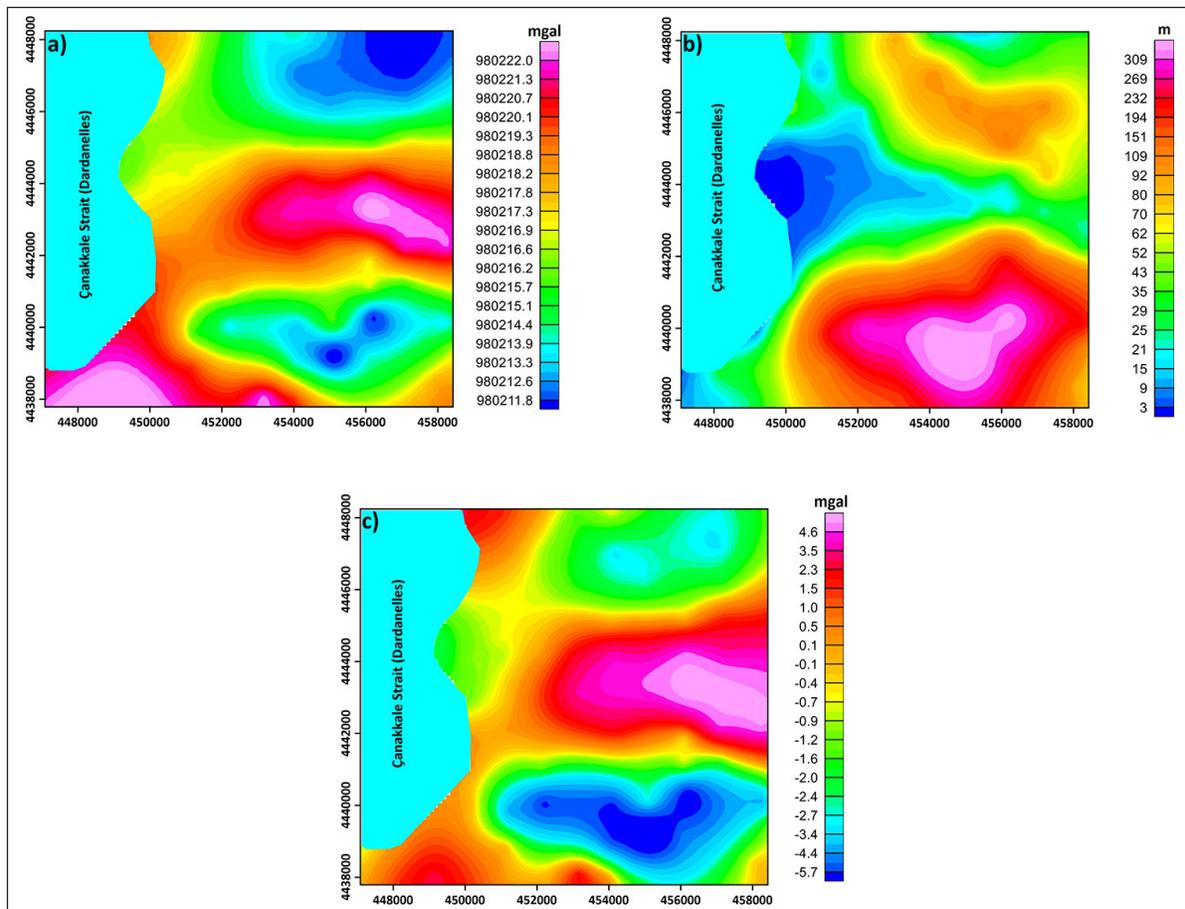
was obtained (Figure 5b). The Ulupınar hill, which has the lowest gravity value (-10 to -13 mGal) in the southeast of the area, stands out most clearly on the map. The height of this place reaches around 430 m. Gravity measurement values include regional values. The regional effect complicates the processing of gravity data by potential field data evaluation methods. Therefore, it is necessary to obtain residual anomaly data by eliminating the regional effect in the data. One of the techniques used in the differentiation of regional-residual anomalies is trend analysis. This analysis can be linear, orthogonal etc. done with polynomials. In this study, residual anomalies were obtained by removing the first-degree trend to the Bouguer Gravity Anomaly. The first-order de-trended gravity anomalies are shown in Figure 5c.

The 3D modelling was applied to the Bouguer anomalies obtained from the microgravity measurements made in the study area. In this method, the gravity anomaly is gridded as a rectangle. Each grid point is the centre of the vertical prismatic structure, and the cross-sectional dimensions of the prisms are equal to the grid intervals. In this way, the data is divided into prisms of equal density as the grid point. The method developed by Cordell and Henderson (1968) was applied to the gravity data shown in Figure 5c to determine the change in young alluvium thickness in the study area. The density difference value was taken as (-0.58 gr.cm^{-3}) (bedrock density= 2.8 gr.cm^{-3} and alluvial density=2.22 gr.cm^{-3}) while making three-dimensional modelling. The thickness of the young alluvial unit in the study area was determined to be approximately 300 m at most as can be seen from the 3D depth model. Prismatic representation of the three-dimensional model is given in Figure 6. In this map, it can be said that the basin depth of the study area is in the range of 160-200 m in the city centre of Çanakkale, the bedrock almost outcrops in the east of Sarıçay and the deepest is observed around 40 m in this part.
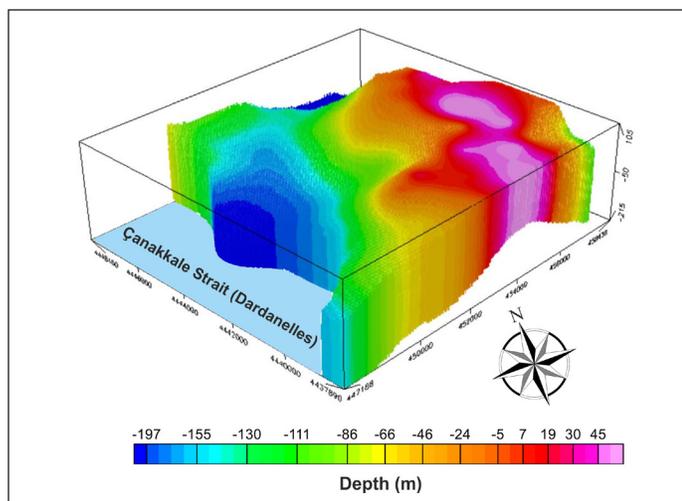
Figure 6. 3D prismatic gravity depth map (After Büyüksaraç *et al.*, 2022)

On the other hand, in the Karacaören Basin in the north of the area, it was observed to be in the range of 200-240 m, with the deepest reaching 240 m.

Inversion of Rayleigh Wave Ellipticity Curve

The local ground response describes the effects on ground motion of shallow sediments, often tens or even hundreds of meters deep, with the slowest seismic velocity. Since soft sediments are limited in size, the affected frequencies are generally higher than 1 Hz. The main factors contributing to the local ground response include impedance effect, non-linear ground content, and potentially resonance effects. Basin effects are related to the deep structure of sediments existing in many areas. Basins generally contain soft sediments near the surface that gradually transition to harder sediments with depth. Topographic effects are related to irregularities in ground surface morphology that can produce local amplification. The frequencies affected by topographic effects depend on the scale of the topographic features.

For example, a local steep hill will affect higher frequencies than large mountains (Stewart *et al.*, 2017).

Shear wave velocity profile and bedrock depth are key parameters for seismic field response estimation. It can be easily determined using geophysical surface wave methods. The surface wave distribution changes along the propagation path depending on the nature of the place where these waves pass. Therefore, surface wave distribution analysis is a good tool to study the most important features of ground structure.

The main advantage of surface wave methods is the ability to characterize the shear wave velocity of the soil on a larger scale. However, in general, the depth of exploration is less than 20 m. A deeper V_s profile is obtained by using the Rayleigh ellipticity curve from active and/or passive measurements. For example, in the Iberian Peninsula, various slip rate models of the crust and upper mantle have been described by Corchete *et al.* (1993, 1995) from the analysis of the Rayleigh wave distribution. This analysis consists of filtering and inversion of the Rayleigh wave distribution to obtain the variation in shear wave velocity versus depth. Sexton *et al.* (1977) showed that the Rayleigh wave ellipticity mainly depends on the local shell structure and does not exhibit azimuth dependence in the range of 10 - 50 seconds.

Therefore, the observed ellipticity for this period range is primarily controlled by the local crustal geology below the seismic station and is not dependent on the propagation path of Rayleigh waves. This essential feature of ellipticity means that ellipticity analysis is a very useful tool for obtaining local crustal models that can be used to identify site and/or local effects in seismic risk and/or seismic design studies (Lee *et al.*, 2003; Rastogi *et al.*, 2011). The ellipticity curve depends on the soil structure and corresponds to the ratio between the

horizontal and vertical components of the ellipse, defined by the particle motion of Rayleigh waves as a function of frequency. The Rayleigh ellipticity curve can be obtained from three-component ambient vibration recordings made at a single station (Gouveia *et al.*, 2016). It is known that the observed ellipticity of a Rayleigh wave can be calculated using the Equation (4) (Aki and Richards, 1980).

$$\varepsilon(T) = A_L(T)/A_Z(T) \qquad (4)$$

Here $A_L(T)$ and $A_Z(T)$ are the instrument corrected spectral amplitudes of the longitudinal (also called radial) and vertical seismograms for the period T (Sexton *et al.*, 1977). Rayleigh waves, whose particle motion is in the form of an ellipse and whose motion is opposite to the direction of propagation, propagate in an elastic medium that is semi-infinitely homogeneous. Rayleigh waves are formed by linear interference of P (primary waves) and SV (vertical component of S-wave) waves. In addition, for dispersion to occur in Rayleigh waves, it must propagate in a stratified medium. The phase shift in interference of vertical and horizontal components is $\pm\pi/2$. Depending on whether the phase shift is positive or negative, the particle motion proceeds in the opposite or forward direction. In a homogeneous semi-infinite medium, the particle motion goes backwards at all frequencies and the ellipticity is constant. However, in the case of a stratified environment, the ellipticity is not constant and the particle motion changes from reverse elliptical motion to forward elliptical motion depending on the contrast between bedrock and ground (Konno and Ohmachi, 1998;

Ullah, 2017). The ellipticity can be determined by the H/V spectral ratio between the peak at the fundamental dominant frequency and the first minimum at the high frequency (Fäh *et al.*, 2001). Therefore, using the shape of the H/V spectral ratio, the 1-Dimensional S-wave velocity structure of the earth can be revealed. Accurate results have been obtained in areas where the bedrock is both shallow and deep using this method (Fäh *et al.*, 2001; Parolai *et al.*, 2005). The 1-Dimensional seismic velocity structure of the soil affects the propagation of Rayleigh waves and the shape of the H/V spectral ratios obtained with the help of microtremor measurements in the ground (Picotti *et al.*, 2017). Thus, the 1-Dimensional velocity structure of the soil can be obtained by inverting the ellipticity of Rayleigh waves in the fundamental mode (Fäh *et al.*, 2001; Picotti *et al.*, 2017).

The inversion of the ellipticity curves of Rayleigh waves (Figure 7a) is done using Dinver software from the Geopsy package (www.geopsy.org, Wathelet *et al.*, 2020) based on the neighbourhood algorithm (Figure 7b). The parameters that need to be set before inversion are:

- The number of loose layers on the bedrock
- The variation range of their thickness (hmin, hmax)
- Density (min, max)
- Body wave velocity ranges (V_p and V_s)
- Poisson's ratio

The ellipticity curves of Rayleigh waves alone are not sufficient to correlate the depth and velocity values during inversion. Therefore, such an inversion only works in com-
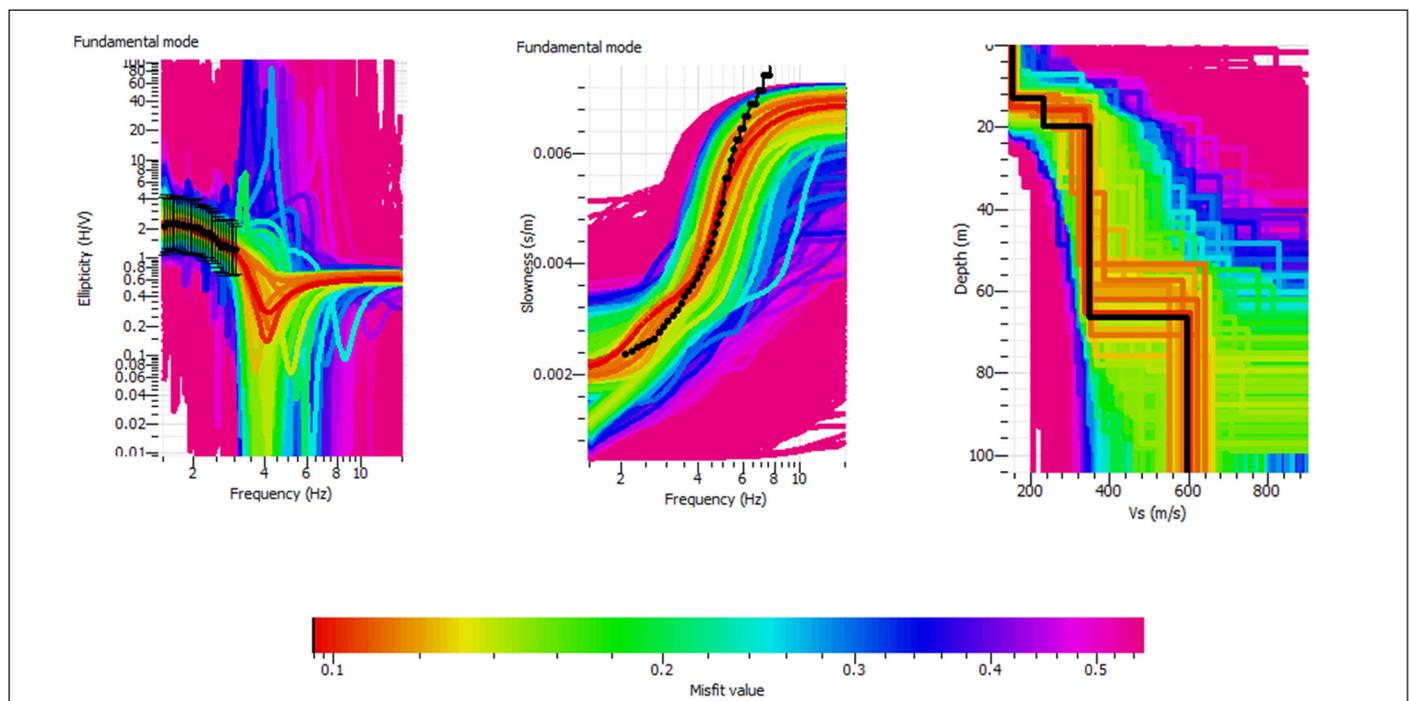
Figure 7 (a). Rayleigh ellipticity graph, (b) Obtaining V_s velocity values, (c) Depth-velocity structure example graph
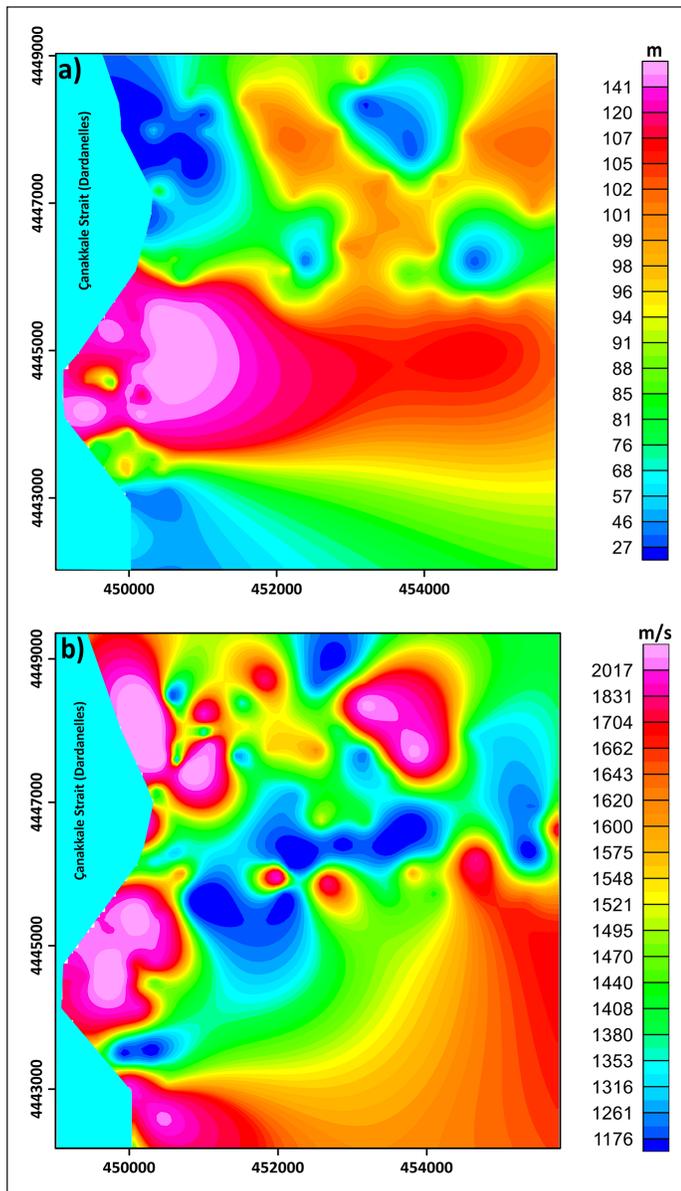
Figure 8 (a). V$_s$ velocity base depth map (includes depth values exceeding 700 m/s velocity value), (b) V$_s$ velocity distribution map under bedrock depth
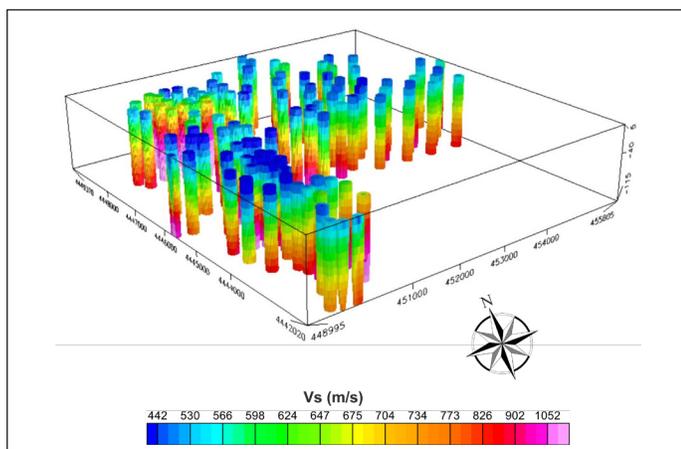
Figure 9. 3D vertical V$_s$ sounding velocity variation map

bination with values obtained from analysis of superficial V$_s$ values such as MASW. Similarly, it is recommended to limit the initial soil model by using previous information (wave velocity, densities, layer thicknesses, etc.) from other geotechnical and geophysical techniques (drilling, seismic fracturing, etc.). The inversion process generates a large number of possible V$_s$ values. For each soil model created, its theoretical curve is calculated and then compared to the experimental one with a false parameter indicating how close the calculated curves are to the experimental ones (Figure 7c).

Rayleigh Ellipticity Calculation and Obtaining S-Wave Velocity

A data set was created by combining microtremor measurements made at 109 points with dispersion curves from which dispersion curves can be obtained, and microtremor measurements made at 37 points within the scope of this project, from the microtremor data collected within the scope of the soil research projects that were made in the study area (Figure 4). Thus, an inverse solution was applied to the generated data via Geopsy software. 1-dimensional V$_s$ velocity and depth values were calculated for the stratified ground structure.

First, a depth map of the study area was created by using V$_s$ values (Figure 8a). This map has been designed as a seismic base map, considering 700 m/s and higher values. The ground structure representing the bedrock or accepted as the seismic basis gives different seismic velocity change values in some parts of the study area. There are very high-speed values as well as limit values. The deepest (below seismic bedrock) V$_s$ seismic velocity distribution map was also created in order to make this distinction (Figure 8b). In addition, a 3-dimensional velocity change map, which can also be defined as V$_s$ sounding, was created by using V$_s$ depth values (Figure 9).

Results and Discussions

Within the scope of this study, which covers the Çanakkale Strait, one of the rare geographies in the world and Turkey's two strait passages, the centre of the city of Çanakkale, which is located on the edge of Çanakkale Strait (Dardanelles), and the nearby towns, a basin depth study based on gravity and microtremor measurements was carried out. Gravity measurements covered a very wide area and depth information about a large part of the Çanakkale Basin could be reached. The entire Bouguer gravity map exhibits anomalies suitable for the geological situation. The region with the lowest negative gravity anomalies (~ -6.0 mGal) is the highest peak in the study area and marine material tempered limestones are dominant. Negative gravity values (~ -2.0 mGal) are also observed in the north-eastern plain uplift. Positive gravity

anomalies were observed on the central quaternary sediments of the study area, as they mostly show marine continental features. The trend removal process was applied to the Bouguer gravity anomalies, and the field was modelled as 3D based on the trend removed gravity anomalies. During the modelling of the gravity anomalies, the density difference between the shallow alluvial units and the volcanic base was considered. Accordingly, modelling was done according to the density difference of -0.58 g/cm³. It was observed that the alluvial thickness of the area increased especially around Sarıçay, which almost divides the city into two, while the alluvial thickness decreased considerably from Sarıçay to the east. The average thickness of alluvium in the north of the basin is around 20-30 m. Karacaören Plain, located in the northeast of the basin, generally presents a thick alluvial structure and shallows are formed in places. In the central settlement of Çanakkale, the current sediment thickness goes deeper than 100 meters. In the southern parts, the alluvium becomes shallow again. Findings confirming the results obtained from the three-dimensional gravity model

were obtained in the 2-dimensional sections created based on the microtremor measurements made in the direction of two separate profiles taken from the south to the north and from the west to the east of the study area. Combined depth sections from both gravity and V_s velocity variations are given in Figures 10a and 10b. Dominant frequency values in these sections were also used as a controller and its compatibility with the behaviour of the basin was observed. In these sections, thicknesses of up to 200 meters can be seen in the parts of Sarıçay close to the Dardanelles. The part of Sarıçay, which is seen as the alluvial fan on the side of the Dardanelles, is the region where alluvium is thickest. On the other hand, the V_s velocity is low due to the shallow groundwater effect in the middle of the basin.

Conclusions

Çanakkale Basin is a Quaternary sedimentary basin dominated by terrestrial and marine alluvial materials. The presence of very loose alluvial materials and shallow groundwater also create important ground problems throughout the basin. The
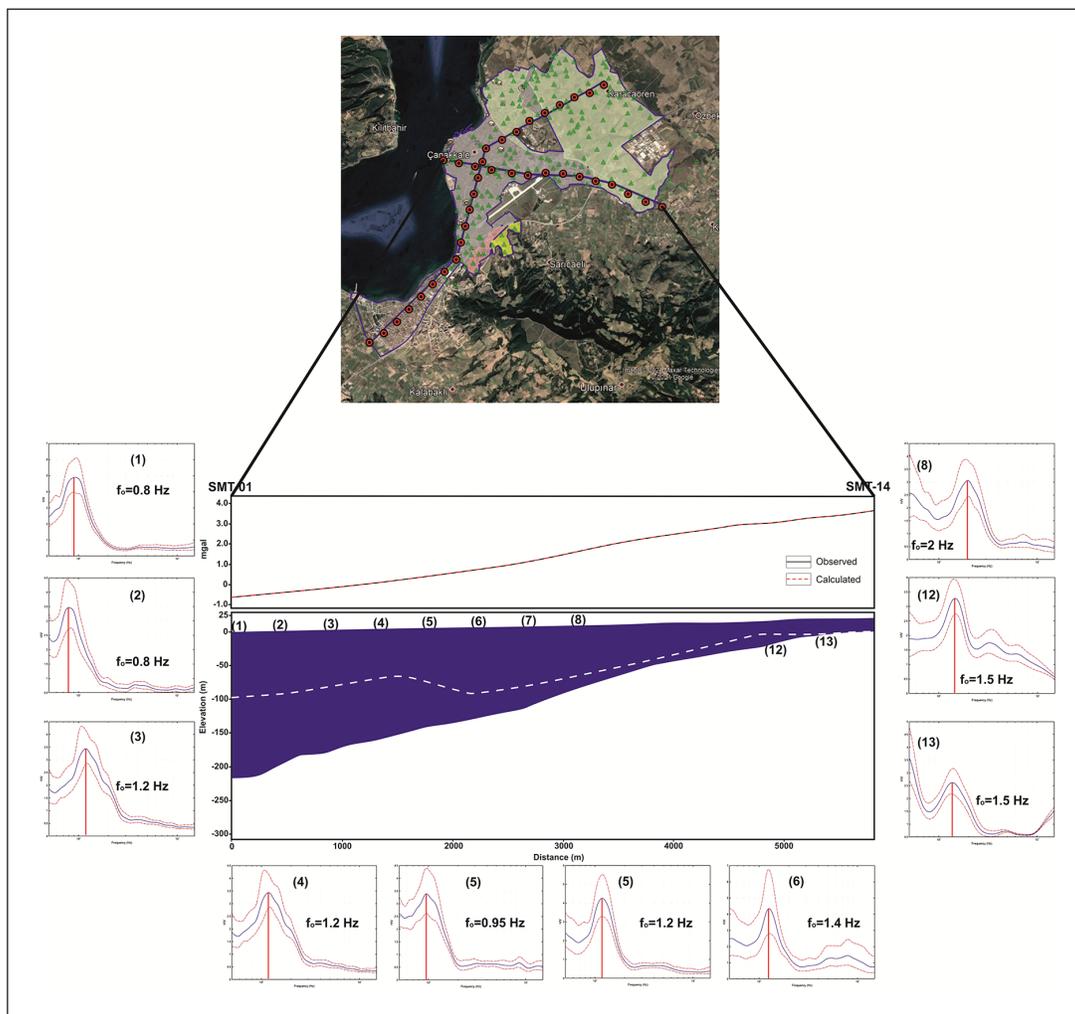
Figure 10 (a). Combined depth section obtained from gravity and V_s-velocity changes along points SMT-01-SMT-14 (White dashed line bedrock boundary obtained from Rayleigh ellipticity measurements ($V_s > 700$ m/s))
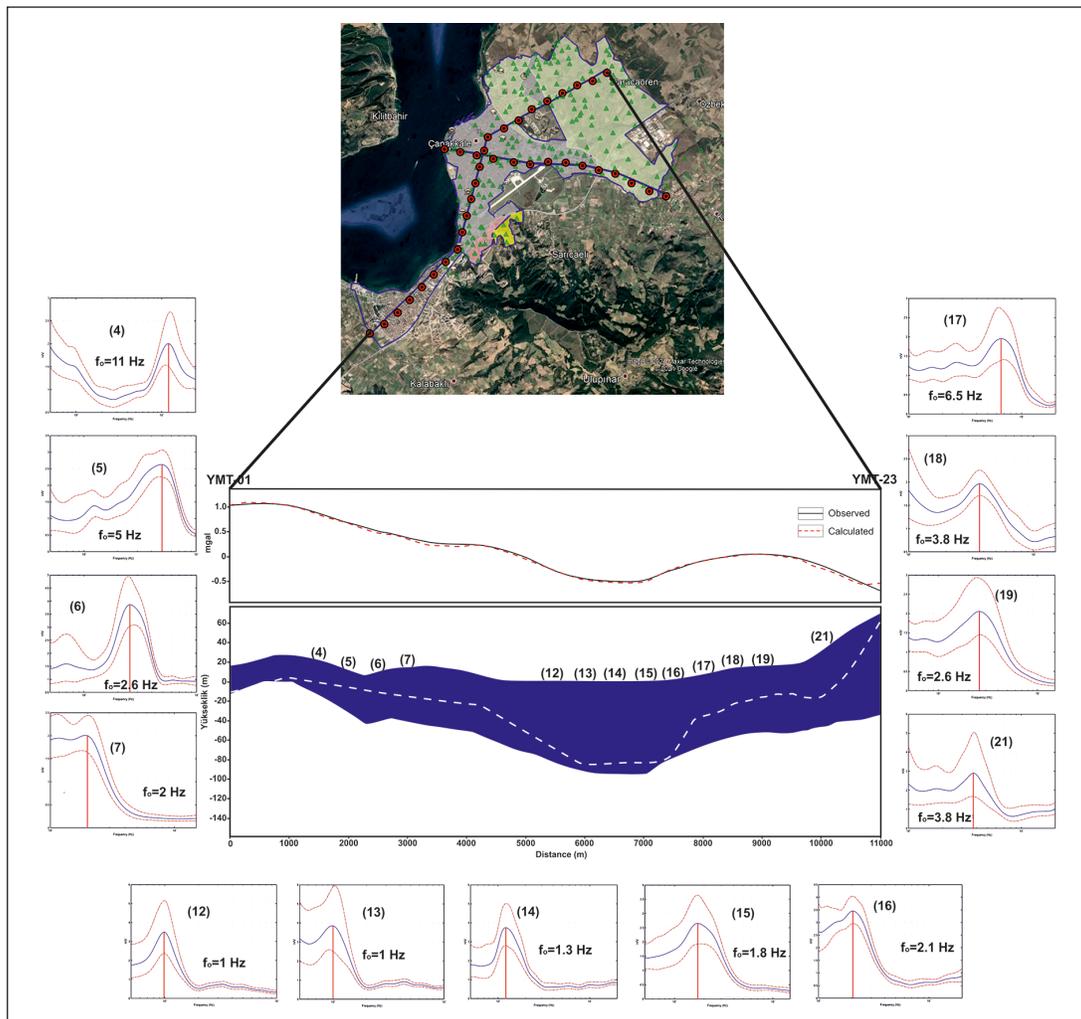
Figure 10 (b). Combined depth section obtained from gravity and velocity variations along points YMT-01-YMT-23 (White dashed line bedrock boundary obtained from Rayleigh ellipticity measurements ($V_s > 700\,m/s$))

fact that there is a dense building settlement on the alluvium requires a holistic planning for the Basin. Important findings have been reached with this study. The basement rock depth of the basin was obtained according to the gravity data, and the engineering foundation depth information was created with microtremor measurements. It has been observed that in areas where the local ground response, V_s velocity decreases and frequencies are relatively low (0.8-1.3 Hz), there are areas with loose, soft sediments. Towards the basin edges, in the sections where the bedrock depth decreases, the V_s velocity increases, and the ground frequency values increase considerably (1.5-11.0 Hz). The thickest part of the basin is Ulupınar hill, which is about 300 m deep and is outside the settlement area. The thickness of the basin reaches approximately 200 meters in the alluvial fan, where the settlement is dense, on the edge of the Çanakkale Strait (Dardanelles) and where the Sarıçay River empties into the sea. The southern and eastern parts of the basin are shallow, while the northern and western parts are deeper. V_s velocity values are quite low in the first 10 meters and increase after 10 meters. In the

study, the definition of V_s sounding was also made throughout the Basin. With this study, loose basin material thickness and local ground response information, which are the basic information of seismic safe settlement in a basin, were revealed as a whole. Based on this information, the expected acceleration values in the basin, repetitive reflection effects near the basin edge and possible soil amplification effects can be calculated.

Acknowledgements

References

Akkaya İ., Özvan A., 2019, Site characterization in the Van settlement (Eastern Turkey) using surface waves and HVSR microtremor methods.

Journal of Applied Geophysics.160, 157-170. **https://doi.org/10.1016/j.jappgeo.2018.11.009**

Aki K. and Richards P. G., 1980, Quantitative seismology: Theory and methods, v.l: W.H. Freeman and Co.

Anbazhagan P., Janarthana Boobalan A., Shaivan H.S., 2019, Establishing empirical correlation between sediment thickness and resonant frequency using HVSR for the Indo-Gangetic Plain. Current Science. 117(9), 1482-1491. **https://doi.org/10.18520/cs/v117/i9/1482-1491**

Atabey E., Ilgar A. ve Sakıtaş A., 2004, Çanakkale Havzasının Orta – Üst Miosen Stratigrafisi, Çanakkale, KB Türkiye. MTA Dergisi,128: 79-97.

Ateş A., Büyüksaraç A., Bilim F., Bektaş Ö., Şendur Ç., Komanovalı G., 2009, Spatial correlation of the aeromagnetic anomalies and seismogenic faults in the Marmara region, NW Turkey, Tectonophysics, 478 (1-2), 135-142. **https://doi.org/10.1016/j.tecto.2008.09.025**

Barka A.A., 1997, Neotectonics of the Marmara region in active tectonics of Northwest Anatolia. C. Schindler, M. Pfister (Eds.), The Marmara Poly-project, Hochschulverlag AG an der ETH, Zurich, pp. 55-87.

Bekler T., Demirci A., Ekinci Y.L., Büyüksaraç A., 2019, Analysis of local site conditions through geophysical parameters at a city under earthquake threat: Çanakkale, NW Turkey. J Appl Geophys, 63, 31-39. **https://doi.org/10.1016/j.jappgeo.2019.02.009**

Birgören G., Özel O., Siyahi B., 2009, Bedrock depth mapping of the coast south of Istanbul: Comparison of analytical and experimental analyses. Turkish J Earth Sci, 18, 315–329. **https://doi.org/10.3906/yer-0712-3**

Birkle P. ve Satır M., 1995, Dating, Geochemistry and geodynamic significance of the Tertiary magmatism of the Biga Peninsula, NW-Turkey. Geology of the Black Sea Region, Min. Res. Expl. Inst. of Turkey, Ankara, pp. 171-180.

Büyüksaraç A., Bektaş O., Yılmaz H., Arısoy M.O., 2013, Preliminary seismic microzonation of Sivas city Turkey using microtremor and refraction microtremor (ReMi) measurements. J. Seismol. 17, 425–435. **https://doi.org/10.1007/s10950-012-9328-1**

Büyüksaraç A., Bekler T., Demirci A., Eyisüren O., 2021, New insights into the dynamic characteristics of alluvial media under the earthquake prone area: a case study for the Çanakkale city settlement (NW of Turkey) Arabian Journal of Geosciences, 14:2086 **https://doi.org/10.1007/s12517-021-08430-3**

Büyüksaraç, A., Karaca, Ö., Eyisüren, O., Bektaş, Ö., Işık, E., 2022, Importance of Bedrock Depth Knowledge in Basins: Çanakkale (Dardanelles) Case History. In: Glavaš, H., Hadzima-Nyarko, M., Karakašić, M., Ademović, N., Avdaković, S. (eds) 30th International Conference on Organization and Technology of Maintenance (OTO 2021). OTO 2021. Lecture Notes in Networks and Systems, vol 369. Springer, Cham. **https://doi.org/10.1007/978-3-030-92851-3_25**

Corchete V., Badal J., Pujades L. and Canas J. A., 1993, Shear velocity structure beneath the Iberian Massif from broadband Rayleigh wave data. Phys. Earth Planet. Inter., 79, 349-365. **https://doi.org/10.1007/s00531-010-0581-7**

Corchete V., Badal J., Serón F. J. and Soria A., 1995, Tomographic images of the Iberian subcrustal lithosphere and asthenosphere. Journal of Geophysical Research, 100, 24133-24146. **https://doi.org/10.1029/95JB00979**

D'Amico V., Picozzi M., Baliva F., Albarello D., 2008, Ambient Noise Measurements for Preliminary Site-Effects Characterization in the Urban Area of Florence, Italy. Bulletin of Seismological Society America, 98 (3), 1373–1388. **https://doi.org/10.1785/0120070231**

Delgado J., Casado C. L., Estevez A., Giner J., Cuenca A., Molina S., 2000a, Mapping soft soils in the Segura River valley (SE Spain): A case study of microtremors as an exploration tool. Journal of Applied Geophysics, 45, 19–32. **https://doi.org/10.1016/S0926-9851(00)00016-1**

Del Monaco F., Tallini M., De Rose C., Durante F., 2013, HVNSR survey in historical downtown L'Aquila (central Italy): Site resonance properties vs. subsoil model. Engineering Geology, 158, 34–47. **https://doi.org/10.1016/j.enggeo.2013.03.008**

Duru M. Pehlivan Ş. Aral İ. O. Şentürk Y. Yavaş F. Kar H., 2012, Biga Yarımadasının Tersiyer Öncesi Jeolojisi, Maden Tetkik ve Arama Genel Müdürlüğü Yayınları, Özel Yayınlar Serisi, No 28: 7-74.

Fah D., Kind F., Giardini D., 2001, A theoretical investigation of average H/V ratios. Geophys J Int, 145, 535–549. **https://doi.org/10.1046/j.0956-540x.2001.01406.x**

Fairchild G.M., Lane J.W., Voytek E.B., LeBlanc D.R., 2013, Bedrock topography of western Cape Cod, Massachusetts, based on bedrock altitudes from geologic borings and analysis of ambient seismic noise by the horizontal-to-vertical spectral-ratio method, U.S. Geological Survey Scientific Investigations Map 3233, 1 sheet, maps variously scaled, p 17. Pamphlet, on one CD–ROM. **http://pubs.usgs.gov/sim/3233. Accessed** 20 Feb 2017.

García-Jerez A., Luzón F., Navarro M., Pérez-Ruiz A., 2006, Characterization of the Sedimentary Cover of the Zafarraya Basin, Southern Spain, by Means of Ambient Noise. Bulletine of Seismological Society America, 96(3), 957–967. **https://doi.org/10.1785/0120050061**

Genç Ş.C. ve Yılmaz Y., 1994, Post Collisional Magmatism in Armutlu Peninsula, NW Anatolia: IAVCEI International Volcanology Congress, Abstracts, Ankara.

Gouveia F., Lopes I., Gomes R.C., 2016, Deeper VS profile from joint analysis of Rayleigh wave data. Engineering Geology, 202, 85–98. **https://doi.org/10.1016/j.enggeo.2016.01.006**

Harutoonian P., Leo C.J., Tokeshi K., Doanh T., Castellaro S., Zou J.J., 2013, Investigation of dynamically compacted ground by HVSR-based approach. Soil Dynamics and Earthquake Engineering, 46, 20–29. **https://doi.org/10.1016/j.soildyn.2012.12.004**

Hinzen K.G., Weber B., Scherbaum F., 2004, On the resolution of H/V measurements to determine sediment thickness, a case study across a normal fault in the Lower Rhine Embayment, Germany. Journal of Earthquake Engineering, 8(6), 909-926. **https://doi.org/10.1142/S136324690400178X**

Ilgar A., Demirci E.S., Duru M., Pehlivan Ş., Dönmez M., Akçay A. E., 2008, 1/100.000 ölçekli Türkiye Jeoloji Haritaları Çanakkale H15 ve H16 Paftaları. No: 100. Maden Tetkik ve Arama Genel Müdürlüğü, Ankara.

Ilgar A., Demirci E.S., Demirci Ö., 2012, Biga Yarımadası Tersiyer istifinin stratigrafisi ve sedimantolojisi. Biga Yarımadası'nın Genel ve Ekonomik Jeolojisi, Editörler: Erdoğan Yüzer, Gürkan Tunay, Maden Tetkik ve Arama Genel Müdürlüğü Özel Yayın Serisi

Kamalian M., Jafari M.K., Ghayamghamian M.R., Shafiee A., Hamzehloo H., Haghshenas E., Sohrabi-bidar A., 2008, Site effect microzonation of Qom, Iran, Engineering Geology, 97 (1–2), 63-79. **https://doi.org/10.1016/j.enggeo.2007.12.006**

Karacık Z., Yılmaz Y., 1998, Geology of the Ignimbrites and the Associated Volcano-plutonic Complex of the Ezine Area, northwestern Anatolia, Journal of Volcanology and Geothermal Research, 85, 251-264. **https://doi.org/10.1016/S0377-0273(98)00058-4**

Kolat Ç., Doyuran V., Ayday C., Süzen M. L., 2006, Preparation of a geotechnical microzonation model using Geographical Information Systems based on Multicriteria Decision Analysis, Engineering Geology, 87(3–4), 241-255. **https://doi.org/10.1016/j.enggeo.2006.07.005**

Konno K., Ohmachi T., 1998, Ground-Motion Characteristics Estimated from Spectral Ratio between Horizontal and Vertical Components of Microtremor. Bull. Seism. Soc. Am., 88, 228-241. **https://doi.org/10.1785/BSSA0880010228**

Kuo C., Chen C., Lin C., Wen K., Huang J., Chang S.J., 2016, S-wave velocity structure and site effect parameters derived from microtremor arrays in the Western Plain of Taiwan. J Asian Earth Sci, 128(1): 27-41. **https://doi.org/10.1016/j.jseaes.2016.07.012**

Kürçer A., Chatzipetros A., Tutkun S.Z., Pavlides S., Ateş Ö., Valkaniotis S., 2008, The Yenice–Gönen active fault (NW Turkey): Active tectonics and palaeoseismology. Tectonophysics, 453(1–4): 263–275. **https://doi.org/10.1016/j.tecto.2007.07.010**

Lee W., Kanamori H., Jennings P. and Kisslinger C., 2003, International Handbook of Earthquake and Engineering Seismology. Elsevier, New York.

Le Pichon X. and Kreemer C., 2010, The Miocene-to-Present Kinematic Evolution of the Eastern Mediterranean and Middle East and Its Implications for Dynamics, Annual Review of Earth and Planetary Sciences 38:1, 323-351. **https://doi.org/10.1146/annurev-earth-040809-152419**

Liang D., Gan F., Zhang W., Jia L., 2018, The application of HVSR method in detecting sediment thickness in karst collapse area of Pearl River Delta, China. Environmental Earth Sciences, 77, 259. **https://doi.org/10.1007/s12665-018-7439-x**

Maghami S., Sohrabi-Bidar A., Bignardi S., Zarean A., Kamalian M., 2021, Extracting the shear wave velocity structure of deep alluviums of "Qom" Basin (Iran) employing HVSR inversion of microtremor recordings. Journal of Applied Geophysics, 104246. **https://doi.org/10.1016/j.jappgeo.2020.104246**

McKenzie D., 1978, Active tectonics of the Alpine-Himalayan Belt: the Aegean Sea and surrounding regions (Tectonics of Aegean Region). Geophysical Journal 55, 217-254. **https://doi.org/10.1111/j.1365-246X.1978.tb04759.x**

Molnar S., Cassidy J.F., Castellaro S., Cornou C., Crow H., Hunter J.A., Matsushima S., Sánchez-Sesma F.J., Yong A., 2018, Application of Microtremor Horizontal-to-Vertical Spectral Ratio (MHVSR) Analysis for Site Characterization: State of the Art. Surveys in Geophysics, 39, 613–631. **https://doi.org/10.1007/s10712-018-9464-4**

Moon S.W., Subramaniam P., Zhang Y., Vinoth G., Ku T., 2019, Bedrock depth evaluation using microtremor measurement: empirical guidelines at weathered granite formation in Singapore. J Appl Geoph, 171: 103866. **https://doi.org/10.1016/j.jappgeo.2019.103866**

Mendecki M.J., Bieta B., Mycka M., 2014, Determination of the resonance frequency – thickness relation based on theambient seismic noise records from Upper Silesia Coal Basin. Contemp. Trends. Geosci.,3, 41-51. **https://doi.org/10.2478/ctg-2014-0021**

Nakamura Y., 2000, Clear identification of fundamental idea of Nakamura's technique and its application", in Proceedings of the XII world conference earthquake engineering. Auckland, New Zeeland, 8 pp.

Över S., Büyüksaraç A., Bektaş O. and Filazi A., 2011, Assessment of potential seismic hazard and site effect in Antakya (Hatay Province), SE Turkey. Environ Earth Sci, 62, 313-326. **https://doi.org/10.1007/s12665-010-0525-3**

Özalaybey S., Zor E., Ergintav S., Tapırdamaz M.C., 2011, Investigation of 3-D basin structures in the Izmit Bay area (Turkey) by single-station microtremor and gravimetric methods. Geophysical Journal International, 186, 883–894. **https://doi.org/10.1111/j.1365-246X.2011.05085.x**

Parolai, S., Picozzi, M., Richwalski, S. M. and Milkereit, C., 2005, Joint inversion of phase velocity dispersionand H/V ratio curves from seismic noise recordings using agenetic algorithm, considering higher modes, Geophys. Res. Lett., 3 2,L01303. **https://doi.org/10.1029/2004GL021115**

Picotti S., Francese R., Giorgi M., Pettenati F. and Carcione J. M., 2017, Estimation of glaciers thicknesses and basal properties using the horizontal-to-vertical component spectral ratio (HVSR) technique from passive seismic data. Journal of Glaciology, 63, 229-248. **https://doi.org/10.1017/jog.2016.135**

Rastogi B.K., Singh A. P., B. Sairam, Jain S. K., Kaneko F., Segawa S. and Matsuo J., 2011, The Possibility of Site Effects: The Anjar Case, Following the Past Earthquakes in the Gujarat, India. Seismological Research Letters, 82(1), 692-701; **https://doi.org/10.1785/** gssrl.82.1.692.

Rupar L., Gosar A., 2020, Mapping the Thickness of Quaternary Sediments in the Iška Alluvial Fan (Central Slovenia) Usıng Microtremor Method. Acta Geodynamica et Geomaterialia, 17(2) (198), 177–190. **https://doi.org/10.13168/AGG.2020.0013**

Sant D.A., Parvez I.A., Rangarajan G., Patel S.J., Bhatt M.N., Salam T.A.S., 2017, Subsurface profiling along Banni Plains and bounding faults, Kachchh, Western India using microtremors method. Journal of Asian Earth Sciences, 146, 326–336. **https://doi.org/10.1016/j.jseaes.2017.06.002**

Sexton J. L., Rudman A. J. and Mead J., 1977, Ellipticity of Rayleigh waves recorded in the Midwest. Bull. Seism. Soc. Am., 67, 369-382. **https://doi.org/10.1785/BSSA0670020369**

Siyako M., Bürkan K.A. ve Okay A.I., 1989, Biga ve Gelibolu yarımadalarının Tersiyer jeolojisi ve hidrokarbon olanakları Türkiye Petrol Jeologları Derneği Bülteni, 1, pp. 183-199, Ankara.

Siyako M., 2006, Trakya Bölgesi Litostratigrafi Birimleri, Stratigrafi Komitesi Litostratigrafi Birimleri Serisi-2. 83 s.

Stewart J.P., Afshari K., Goulet C.A., 2017, Non-Ergodic Site Response in Seismic Hazard Analysis. Earthquake Spectra. 33(4):1385-1414. **https://doi.org/10.1193/081716eqs135m**

Şengör A. M. C., Görür N., Şaroğlu F., 1985, Strikeslip faulting and related basin formation in zones of tectonic escape: Turkey as a case study. (Strike-slip Deformation, Basin Formation, and Sedimentation,

Editörler: Biddle, K.T., ChrisiteBlick, N.). Society of Economic Pale-ontologists and Mineralogists, Special Publication, 227- 264.

Şentürk K. and Karaköse C., 1987, Çanakkale Boğazı ve dolayının jeolojisi, MTA Genel Müdürlüğü, Jeoloji Etüdleri Dairesi Arşivi, yayınlanmamış teknik rapor, 371, 207 s.

Thabet M., 2019, Site-Specific Relationships between Bedrock Depth and HVSR Fundamental Resonance Frequency Using KiK-NET Data from Japan. Pure Appl Geophys. **https://doi.org/10.1007/s00024-019-02256-7**

Tunusluoğlu M. C. and Karaca Ö., 2018, Liquefaction severity mapping based on SPT data: a case study in Canakkale city (NW Turkey), En-vironmental Earth Sciences, 77(12). **https://doi.org/10.1007/s12665-018-7597-x**

Ullah I., 2017, Near-surface characterization from the H/V spectral curves along with the joint inversion of the ellipticity and dispersion curves. Doktora Tezi, São Paulo Üniversitesi, Brezilya.

Wathelet M., Chatelain, J. L., Cornou, C., Di Giulio, G., Guillier, B., Ohrnberger, M., Savvaidis, A., 2020, Geopsy: A User-Friendly open-source tool set for ambient vibration processing, Seismological Research Letters, 91(3), 1878-1889.

Yiğitbaş E., 2016, Jeolojik – Antropojenik Sebep – Sonuç İlişkileri Açısından Çanakkale